

AN EXPERIMENTAL AND NUMERICAL STUDY OF THE SMOKE VENTILATION IN ATRIUM FIRES UNDER DYNAMIC VENTILATION PERFORMANCE

Ayala P.^{a*}, Cantizano A.^a, Gutiérrez-Montes, C.^b

^a Instituto de Investigación Tecnológica, Escuela Técnica Superior de Ingeniería, Universidad Pontificia Comillas, Madrid, Spain

^b Fluid Dynamics Division of the Department of Mining and Mechanical Engineering, Universidad de Jaén, Jaén, Spain

*Author for correspondence
Department of Mechanical Engineering,
Comillas Pontifical University,
Madrid, 28015,
Spain,
E-mail: pablo.ayala@iit.upcomillas.es

ABSTRACT

Smoke control systems within fire safety designs are being commonly investigated by means of computation fluid dynamics (CFD) models due to the increment of accuracy and computational speed. This paper presents a full-scale experimental and numerical comparison of atrium fires of 2.3-2.7 MW and 5.1-5.3 MW using Fire Dynamic Simulator (FDSv6). Results from six different fire tests with dynamic and constant exhaust flow rates during the fire are presented. Different mesh element sizes as well as turbulence models (Deardorff, Dynamic Smagorinsky and Smagorinsky models) assessing the smoke layer interface are compared presenting differences in the steady state of 20% and 10%, respectively. A good agreement is obtained numerically, being the average relative error during the whole experiment of 12% and 17% in low and high heat release rates, respectively. Finally, the smoke layer has been well predicted not only under constant flow rates but also under dynamic flow rates, being the numerical temporal response to the exhaust changes conducted slower than the experimental one.

INTRODUCTION

In case of fires within large volume spaces, such as malls or interchange stations, in which many people are involved, the smoke has to be controlled by means of an exhaust system, being the mechanical exhaust systems the most commonly used ones. The non-exhausted smoke travels long distances as no vertical barriers exist and it is accumulated under the roof differentiating two zones in the volume space: a free-smoke area and the smoke layer. The location of the interface between these two zones, known as smoke layer interface, is the major concern in smoke control designs, [1]. Nowadays, the

improvement of technology achieved in fire protection installations allows to optimize the smoke layer interface control by means of an active management on the extraction velocity, known as dynamic ventilation. There are a few studies related to smoke layer management during the fire, e.g. the study of the benefits of the introduction of a delay between the smoke detection and the fan activation.

Nowadays, the use of computational models (CFD) to predict fire dynamics and smoke movement is boosted being Fire Dynamic Simulator (FDS) the most used, [2]. Different numerical models, such as combustion, turbulence or heat transfer models, among others, are employed and defined by different constants. In atria, the smoke production is determined mainly by the air entrainment into the fire plume, which is numerically highly dependent on the turbulence model and the mesh size, [3]. Moreover, these numerical models have to be validated, e.g. with full-scale experimental fire tests. To this aim, a new set of full-scale fire tests carried out in the Fire Atrium located in Spain, figure 1, is used as a benchmark for the simulations predicting the smoke layer drop by means of temperature comparisons at different locations.

This paper presents an experimental-numerical comparison assessing the smoke exhaust management under constant and dynamic ventilation conditions in order to establish an intervention protocol in case of a fire incident. Therefore, the influence of the mechanical exhaust flow rate on the smoke layer interface is studied under two different system performances: constant flow rate and time dependent extraction rates.

NOMENCLATURE

R^*	[-]	Spatial resolution of the mesh
Δ	[m]	Cell size
z	[m]	Characteristic diameter of the plume
\dot{Q}	[kW]	Heat Release Rate of the fire
ρ_a	[kg/m ³]	Air density
$c_{p,a}$	[J/kgK]	Air specific heat at constant pressure
T_a	[K]	Air temperature
ϕ	[m]	Pool fire diameter
H	[m]	Height
g	[m/s ²]	Gravity
x	[m]	Cartesian axis direction
y	[m]	Cartesian axis direction
z	[m]	Cartesian axis direction

EXPERIMENTAL SET-UP

A new set of full-scale fire tests were carried out in the Fire Atrium, figure 1a, to study the mechanical exhaust system effectiveness, as well as the make-up air supply influence in these kinds of buildings. This facility is a full-scale experimental enclosure of 19.5 x 19.5 x 20 m³ with eight gridded vents distributed in the lowest part of the different walls of the atrium, whose dimensions are 4.88 x 2.5 m². Four fans with two extraction velocities are installed on the roof being the nominal flow rates 4.6 m³/s and 9.2 m³/s, respectively, see figure 1b.

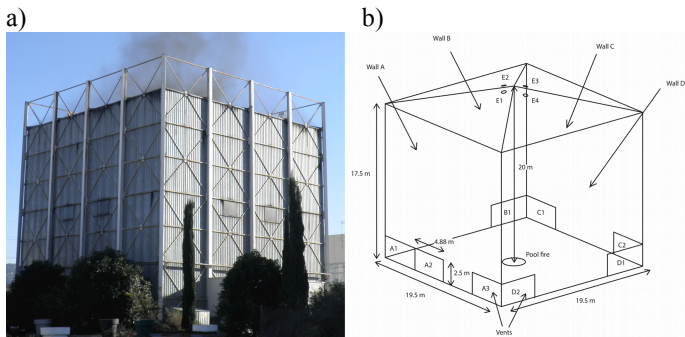


Figure 1 Fire Atrium a), and layout and main dimensions of the atrium b).

During these experiments several measurements were considered: the temperature was measured by means of type K thermocouples; the mass burning rate by three load cells; and the air velocity through the inlet vents with hot-wire anemometers. Fifty-nine thermocouples were distributed at different locations of the atrium, mainly the fire plume, the smoke layer and the far field vertical temperature distribution close to the walls, as can be seen in figure 2. The thermocouple tree, left side of figure 2a, is the one called ‘Smoke Layer’, in which twenty-eight thermocouples were installed along the whole atrium height: from the ground to 5 m high, five thermocouple were installed every meter (sensors 32–36); from 5 to 19 m, twenty thermocouples every half meter (sensors 37–56); and from 15 to 18 m, three thermocouples every meter (sensors 57–59).

Different make-up air supply configurations, extraction flow rates and heat release rates were assessed. Six of these tests are presented herein to study the smoke layer control effectiveness carried out with heptane pools fires in the centre of the atrium and under symmetrical inlet vents distribution, i.e.

vents A1, A3, C1 and C2 were fully opened. On the one hand, the first group, test#1, #2 and #3, were carried out with a pan with a diameter of 1.17 m (2.3 MW). On the other hand, test#4, #5 and #6 were conducted with a pan with a diameter of 1.67 m (5.3 MW). Regarding the exhaust flow rates, test #1 and #4 were carried out with a constant flow rate of 18.3 m³/s during the whole experimental time, whereas test#2 and #5 with 27.5 m³/s. The exhaust flow rate in test#4 and #6 was varied from 18.3 m³/s to 27.5 m³/s during the test at 450 s and 270 s after the ignition, respectively, as can be seen in table 1.

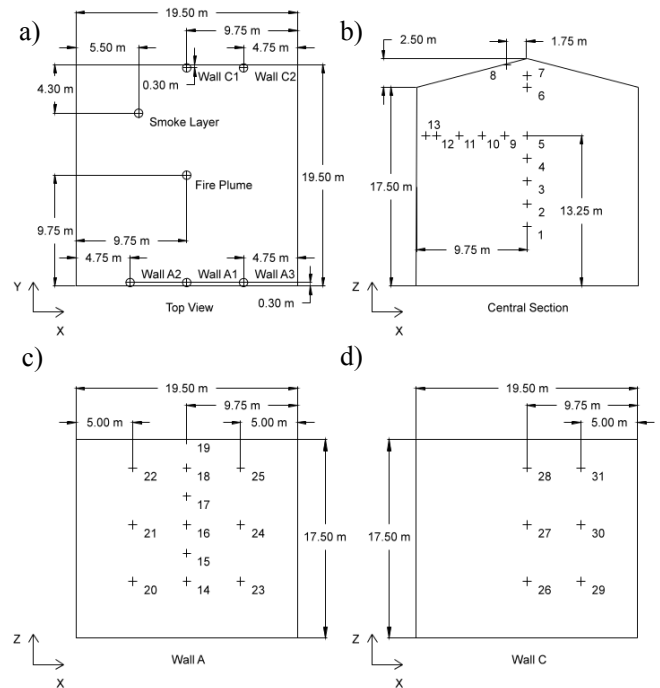


Figure 2 Sensors layout on the atrium: thermocouple trees location, central section (b), at 30 cm from wall A, and at 30 cm from wall C.

Additionally, the three load cells placed under the pan were used to measure the heat release rate. Figure 3 shows the heat release rate of test#1 and #6 with a combustion efficiency established at 92%, as the SFPE organization proposed [4], in which HRR of 2.5MW and 4.8 MW, respectively, were reached during the steady state, i.e. after 200 s.

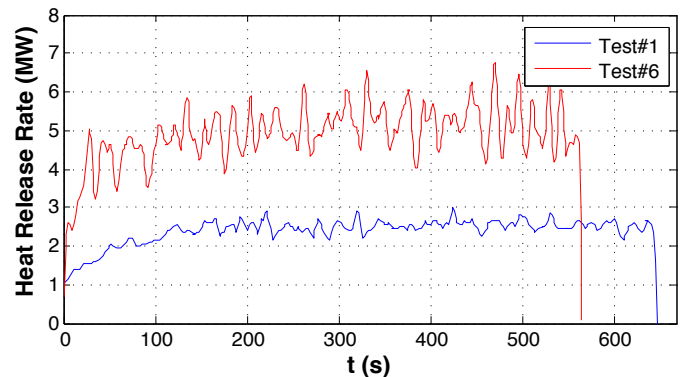


Figure 3 Heat release rate curves of test#1 and test#6.

Table 1 Summary of experimental conditions during the fire tests.

Fire Test	Heptane weight (kg)	Burning time (s)	Open Vents	Exhaust flow rate (m ³ /s)	Ambient temp (°C)	Pressure (Pa)	HRR (MW)
Test#1	36.5	647	A1, A3, C1, C2	18.3	18	101617	2.3
Test#2	36.3	590	A1, A3, C1, C2	27.5	17.5	101617	2.5
Test#3	54.2	836	A1, A3, C1, C2	18.3 – 27.5	19	101617	2.7
Test#4	71	558	A1, A3, C1, C2	18.3	11	102022	5.2
Test#5	73.2	589	A1, A3, C1, C2	27.5	14.9	102191	5.1
Test#6	73	565	A1, A3, C1, C2	18.3 – 27.5	16.7	102191	5.3

NUMERICAL METHOD

AS it has been previously commented, Fire Dynamic Simulator (FDSv6) [2] has been used to carry out the numerical simulations.

Regarding the main models used, a mixture fraction model has been used to simulate the heptane combustion. Therefore, the mass fraction of the reactants as well as products can be obtained from the mixture fraction by means of so called state relations. The fire plume induced by the fire is highly turbulent, being accounted for a large eddy simulation (LES) model, [5]. Furthermore, FDS calculates the directional radiation intensity for non-scattering grey gas and is obtained as a solution of the radiative transfer equation (RTE), [6]. Second order accuracy discretization schemes are used both for the temporal and spatial terms of the governing equations, [3].

The walls and the roof were modelled as 6 mm walls of thick galvanized steel. The ground was simulated as a thick layer of concrete. The fans are introduced as flow rate curves corresponding to the temporal flow rates extracted, and the inlets at the bottom of the atrium as open vents. The outer atmospheric conditions, showed in table 1, are imposed, considering quiescent atmosphere.

The pool fire is modelled setting the estimated Heat Release Rate (HRR) curves as an input as it was described in the Experimental Setup section. The radiation fraction taken in this work for the heptane is 0.35, [7].

Finally, the grid size has to be small enough to model properly the turbulence effects. For the LES method, a spatial resolution between $1/4 < R^* < 1/16$ is recommended, [8]. This spatial resolution is defined as $R^* = \Delta/z$, where Δ is the element size and z the characteristic diameter of the plume, obtained from the Froude number [4], which can be calculated as:

$$z = \left(\frac{\dot{Q}}{\rho_{\infty} c_{p,\infty} T_{\infty} \sqrt{g}} \right)^{2/5} \quad (1)$$

MESH AND TUBULENCE STUDY

During the model validation, it is important to study the influence of the potential elements that can affect the smoke. As the smoke is mainly produced by air entrainment into the fire plume, which depends on the fire plume turbulence and then, by the eddies modelled related with the element size, [3], a sensitivity analysis of the turbulence model used as well as the mesh size influence is presented.

Three uniform cartesian-grids with elements of 10, 13, and 20 cm³, which correspond to meshes of 7.4, 3.4, 0.9 million

elements, respectively, are investigated. Moreover, a mesh with elements of 20 cm³ and a refinement, throughout the whole 6.6 m², with cells of 10 cm³, is assessed. Figures 4a shows the smoke layer drop for the different meshes. The four simulations predict similar smoke layer interfaces being the differences during the last 50 s of simulations lower than 0.7 m (20%), being the most conservative the coarser one (20 cm³). The differences between the simulations with elements of 10 cm³ and 13 cm³ are lower than 8%, not only in smoke layer prediction but also in atrium temperatures, but the computational cost is three times larger, being the second an adequate option to assess the smoke layer interface.

Regarding the turbulence model used, figure 4b, it can be observed that Smagorinsky model with its constant of 0.2 shows a slower smoke layer drop reaching a height of 4.2 m. In the Dynamic Smagorinsky model the smoke travels faster and the smoke layer prediction height is equal to 3.9 m high. Deardorff model prediction is similar to that from Smagorinsky model with its constant of 0.1 or 0.13, which are between the above-mentioned values. Therefore, Deardorff model, which is the default model of FDSv6, [2], can be considered appropriate for this study as well as 0.13 cm as cell size.

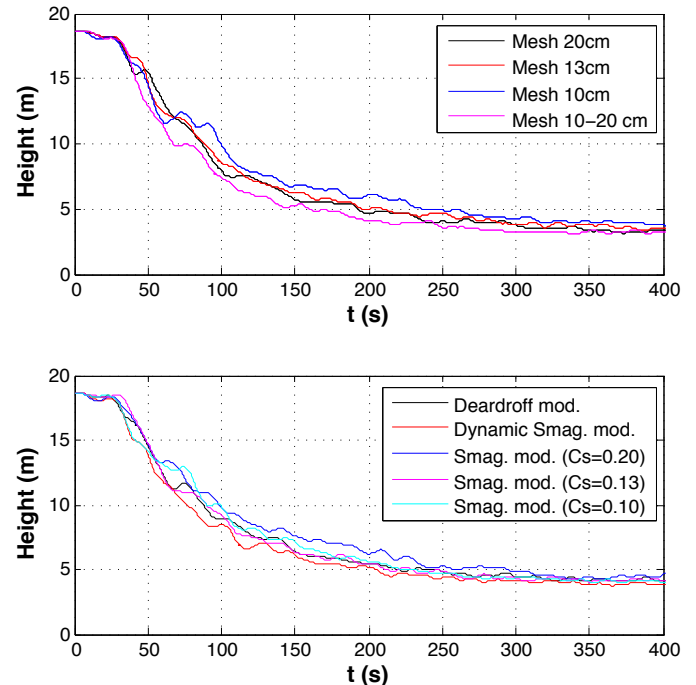


Figure 4 Smoke layer interface under different element sizes a) and under different turbulence models b).

EXPERIMENTAL-NUMERICAL COMPARISON

Pan 34b - $\phi = 1.17\text{m}$

Three fire tests are studied in this paper with the pan 34b which has a diameter of 1.17 m, being the average estimated HRR of 2.4 MW. Test#1 is herein presented in detail to validate the numerical model for this pan size.

Regarding the temperatures at the fire plume (sensors 1-6), Figure 5, thermocouples located closer to the flame show higher oscillations on the temperature profile due to the direct flame influence on them, being difficult to establish a direct comparison. However, the differences of mean values after 300 s of simulation, when it can be considered that the flame reaches a steady state, are equal to 16, 33 and 15 °C, which correspond to 5%, 20% and 14%, at 5.25 m, 7.25 m and 9.25 m high, respectively, figures 5a-c. Also, the temperature predicted at the higher locations, figures 5d-f, is similar to the experiments not only in value but also in shape. These thermocouples are more affected by the smoke layer than by the flame, being their temperature growth slower and reaching the steady state on the last 100 s. The differences in average once the steady state is achieved are equal to 14, 12 and 8 °C, which correspond to 12%, 13%, and 8%, at 12.25, 17.5 and 18.5 m high, respectively.

About the above commented results in figures 5a-f, it can be also observed that the temperature predicted by the numerical models is slightly higher than real measurements.

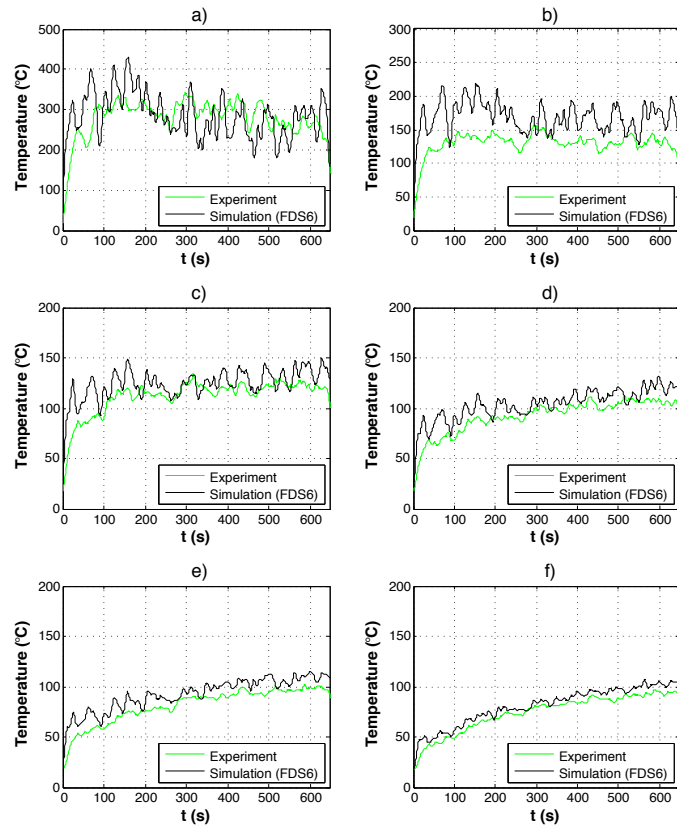


Figure 5 Temperatures on the fire plume in test#1 at h=5.25 m a), h=7.25 m b), h=9.25 m c), h=11.25 m d), h=13.25 m e), and h=17.5 m e).

As for the temperatures recorded close to wall A, figure 6 shows the temperatures predicted experimentally and measured at six thermocouples (sensors 14-19). The temperature is generally well predicted, being the temperature reached higher as the thermocouple is located further from the ground with the exception of the one located near the roof at 17.5 m high, figure 6f, whose temperature is slightly lower than at 15 m high, figure 6e. At 5 m high, it can be observed that the temperature predicted numerically is not steady until 450 s of simulation exceeding the experimental measurements, whereas the experimental temperature is steady after 300 s. Thus, the smoke reaches a lower height as well as travels slightly slower in the simulation. The latter can be also recognized at 7.5 m high, figure 6b, where the temperature does not increase up to 250 s of simulations. As the steady state in the different plots is not reached, a mean value cannot be considered to compare with the numerical model, being more adequate the use of the relative differences at each time step. The largest relative error reached is 30% at 5 m and 7.5 m high at 470 s and 165 s, respectively, being the absolute difference 12.5 °C and 13.5 °C, respectively. The differences in the thermocouples located above those are lower than 7%.

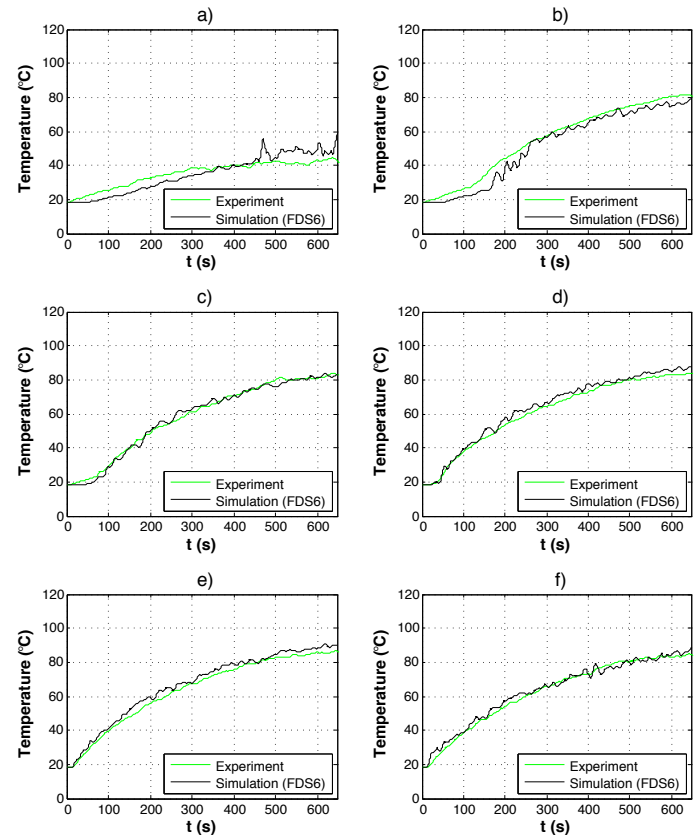


Figure 6 Temperatures at 30 cm from Wall A in test#1 at h=5.0 m a), h=7.5 m b), h=10.0 m c), h=12.5 m d), h=15.0 m e), and h=17.5 m e).

Pan 70b - $\phi = 1.67\text{m}$

Three fire tests were carried out with 70b which has a diameter of 1.67 m, being the averaged estimated HRR of 5.3 MW.

The smoke temperature at different heights of the fire plume can be observed in figure 7. At 5.25, 7.25 and 9.25 m high, figures 7a-c, temperature shows high oscillations due to flame influence, as it was described in test#1. Assessing the average temperature once the HRR reaches the steady state, i.e. after 200 s, the discrepancies between the measurements and the simulations are 10%, 9% and 7% respectively. Above 9.25 m high, figures 7d-f, the temperature is well predicted being the maximum relative error after 450 s, when the steady state is reached, of 31%, and 28%, and 19%, respectively, which corresponds to 40, 26 and 24 °C, and the averaged relative error of 12%, 7% and 11%.

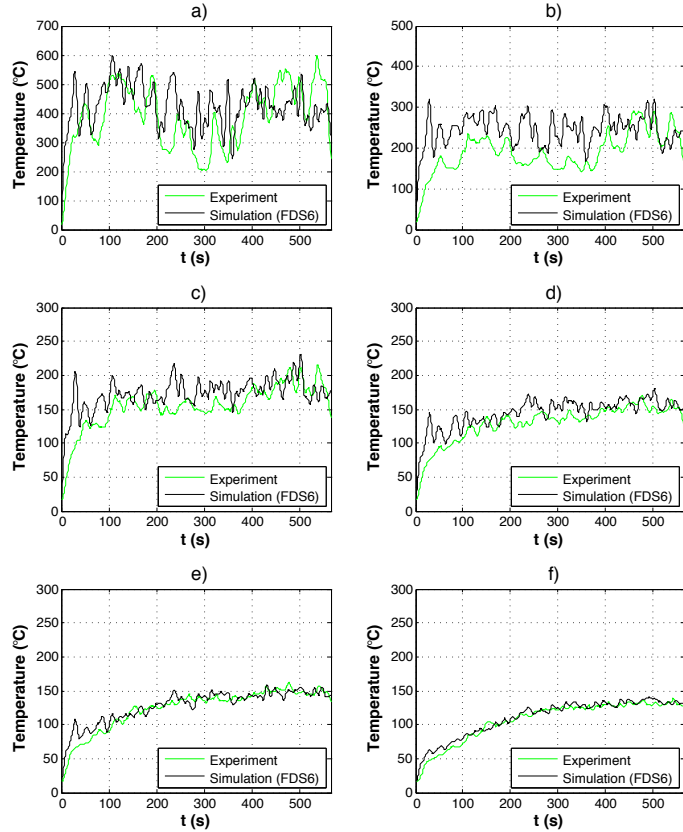


Figure 7 Temperatures on the fire plume in test#6 at h=5.25 m a), h=7.25 m b), h=9.25 m c), h=11.25 m d), h=13.25 m e), and h=17.5 m f).

On the other hand, it can be noticed that close to wall A the temperature is well predicted at the different heights being slightly under predicted. The discrepancies once the steady state is reached looking at these graphs, i.e. after 450 s, are 10%, 17%, 14%, 8%, 6% and 13% in figures 8a-f, being in terms of temperature 1.5, 19, 15, 9, 7.5 and 15 °C, respectively. Moreover, looking at the thermocouple at 5 m high, figure 8a, it can be seen the temperature drop after the 270 s when the flow exhaust rate is changed from 18 m³/s to 27.5 m³/s.

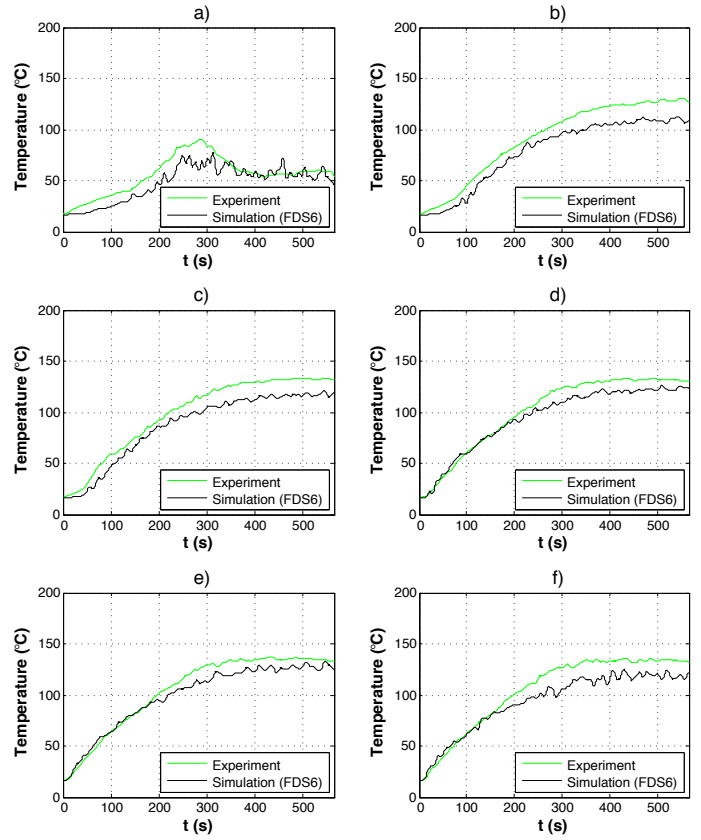


Figure 8 Temperature at 30 cm from Wall A in test#6 at h=5.0 m a), h=7.5 m b), h=10.0 m c), h=12.5 m d), h=15.0 m e), and h=17.5 m f).

VENTILATION PROTOCOL

The smoke layer interface can be assessed by means of CO₂ concentration as well as temperature measurements, being the latter the most used due to the straightforwardness of its measurement in fire safety. Different temperature methods to evaluate the smoke layer interface can be found in the literature such as N-percent method proposed by Cooper et al. [9], the upper zone averaging and mass equivalency by Quintere et al. [10], the maximum gradient method by Emmons [4], Jansen Method [11] and Least-squares method by He et al. [12].

Least-square method is used in this paper because it is not dependent on any parameter neither empirical correlations, [12]. This method, applied in the smoke temperature, establishes the smoke layer interface in which the deviation (σ^2) of the temperature at the smoke layer interface is minimum. This deviation is defined as follows:

$$\sigma^2(H) = \frac{1}{H} \int_0^H [T(z) - T_i]^2 dz + \frac{1}{H_i - H} \int_H^{H_i} [T(z) - T_i]^2 dz \quad (2)$$

$$T_i = H_i / \int_0^H \frac{1}{T(z)} dz \quad (3)$$

$$T_i = H_i / \int_0^H \frac{1}{T(z)} dz \quad (4)$$

where H is the smoke layer interface, H_i the total high of the atrium and $T(z)$ the temperature at height z . Therefore, for a given temperature profile along the height, the smoke layer interface H_i is that which minimizes the deviation:

$$\sigma^2(H_i) = \min[\sigma^2(H)] \quad (5)$$

This method should be assessed every time step to obtain the smoke layer descend.

Temperature measurements in the Smoke Layer thermocouple tree have been used to evaluate the smoke layer interface. Ghost thermocouples have been introduced every 10 cm by means of the linearization from the thermocouples originally installed in order to have more accuracy on the smoke layer interface position.

Figures 9a-e show the smoke layer drop of test#1-6, respectively, being test#5 only assessed numerically due to a failure in the data logger recording the smoke layer thermocouple tree measurements. It can be observed that the smoke layer interface can be separated into three main zones: maximum constant height, smoke layer drop and steady smoke layer interface. The maximum constant height is considered as the time the smoke begins to drop drastically. Regarding this time, FDS predicts shorter times (55, 53, 39, 45, 46, and 36 s for test#1 to #6, respectively) than the experiments (67, 67, 80, 65, -, and 57 s for test#1 to #6, respectively), which is totally understandable due to the thermal inertia of the thermocouples. This thermal inertia turns into a delay in the temperature measurements, and then, in the smoke layer drop. Secondly, the smoke layer drop zone is considered since the smoke drastically drops until the equilibrium between the smoke exhaust and production is reached (the steady smoke layer interface), which settles near around 10 m high. Last, the steady smoke layer interface can be considered reached when the smoke layer is maintain steady in the time within a threshold of 10%.

Table 2 shows the smoke layer interface averaged in a determined time interval. Test#1 and #4, which have the same smoke flow exhaust ($18.5 \text{ m}^3/\text{s}$) and different HRR, presents the same smoke layer interface experimentally (6.2 m high), what does not make sense because the larger the HRR is, the larger the smoke layer production. However, looking at figure 9d, it can be observed that the minimum smoke layer height is reached between 250 and 300 s with a height of 4.2 m, which is more realistic and more accurate with the one predicted by FDS at this time (4.4 m) as well as in the end of the test (4.2 m), when the smoke layer ascends up to the height commented before. Regarding the higher smoke flow rate ($27.5 \text{ m}^3/\text{s}$), test#2 predicts similar smoke layer interface experimentally and numerically (7.5 m), being higher than the one predicted numerically in test#5 as it is expected. Finally, the dynamic exhaust flow rates, test#3 and #6, in which the flow rate is $18 \text{ m}^3/\text{s}$ in the beginning until it is changed to $27.5 \text{ m}^3/\text{s}$, are evaluated observing the smoke layer reaction of a flow exhaust change. Experimentally, this reaction can be clearly noted in figures 9c-d, in which once the smoke flow exhaust is increased the smoke layer ascends. In figure 9c, the smoke after 600 s begins again to descend, which is related to a secondary effect of the high smoke exhaust which increases the flow in the inlet

vents bending the flame, and then, increases the smoke production. Numerically and experimentally, the smoke layer heights predicted at the end of the experiment are 7.3 and 7.4 m high, respectively, table 1. Regarding test#6, figure 9e, the smoke layer prediction experimentally is higher than the one predicted numerically, which is related to the thermocouple thermal inertia, with a difference of 1.1 m at the end of the experiment whereas FDS prediction is 0.7 m lower than the experiment before the flow exhaust change (250–300 s).

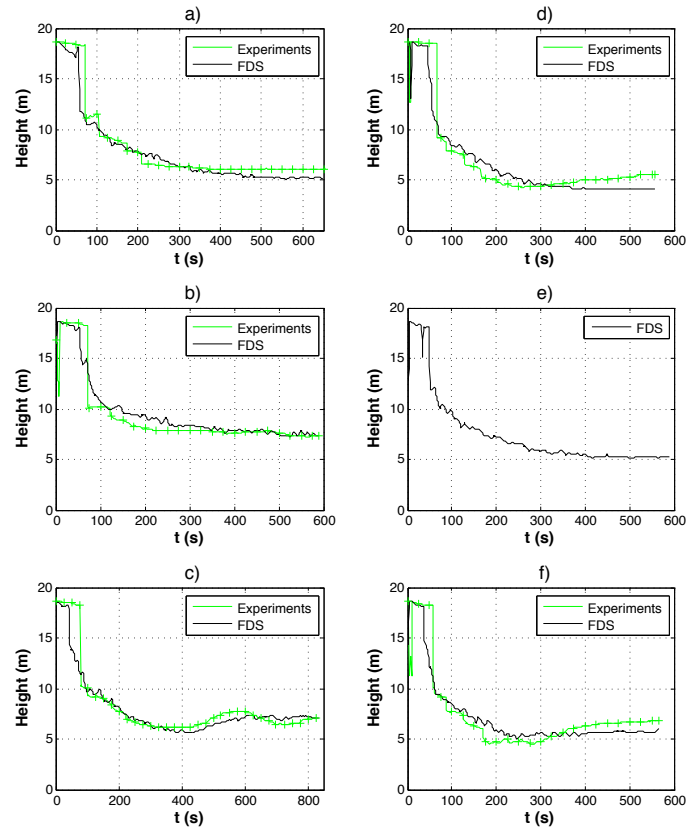


Figure 9: Smoke layer drop in test#1 a), test#2 b), test#3 c), test#4 d), test#5 e) and test#6 f).

Additionally, comparing the experimental results from test#1 and #3, before the smoke flow rate is changed in the latter (450 s), the smoke layer prediction is very similar, 6.2 and 6.3 m, respectively. Moreover, at the end of test#2 and #3 when the smoke flow exhaust is the same, the experimental prediction is again analogous, 7.5 and 7.3 m, respectively. Numerically, it can be concluded the same, being the differences lower than 0.2 m. In addition, comparing experimentally test#4 and #6, before 270 s when the smoke flow rate was changed in the latter, the smoke interface predicted are 4.2 m and 4.8 m, respectively, being larger the numerically prediction difference (1.1 m). And, at the end of test#5 and #6, the numerical predictions are 5.2 m and 5.8 m, respectively.

Table 2 Smoke layer interface.

	Time interval	Smoke layer interface (m)	
		Experiments	FDS
Test#1	400-450 s	6.2	5.7
	Last 100 s	6.2	5.2
Test#2	Last 100 s	7.5	7.5
Test#3	400-450 s	6.3	5.8
	550-600 s	7.8	7.0
	Last 50 s	7.4	7.3
Test#4	250 -300 s	4.2	4.4
	Last 100 s	6.2	4.2
Test#5	Last 100 s	-	5.2
Test#6	250-300 s	4.8	5.5
	Last 50 s	6.9	5.8

CONCLUSIONS

The paper presents the validation of two fire tests of 2.3 MW and 5.3 MW from the six herein presented within a large-scale atrium under different exhaust flow rates (constant flow rate and time dependent extraction rates) in order to study of the smoke layer prediction and behaviour. Additionally, a study of the influence of the mesh size and the turbulence model has been conducted in order to assess their influence on the smoke layer.

A good agreement has been found between the experimental data and numerical simulations not only in the fire plume, but at the far field as well. In the fire plume, the numerical temperature is slightly over-predicted, being clearly affected by the flame, whereas in the far field the differences are lower than 12% in average and 30% in peak. The smoke layer interface is numerically affected by the cell size as well as the turbulence model, finding differences of 20% and 10% when the steady state is reached. Additionally, the smoke layer has been also studied and compared experimentally, observing three different zones: maximum constant height, smoke layer drop and steady smoke layer interface. Dynamic flow exhaust simulations have shown a slower reaction than the experiments reaching conservative predictions.

In summary, it has been clearly observed a direct impact of the flow rate on the smoke layer drop, which would allow to better control the smoke layer descent.

ACKNOWLEDGMENTS

The authors want to acknowledge Dr. Guillermo Rein from Imperial College London for their technical suggestions. This research was supported by Fundación Mapfre under Project # PR/11/AYU/072, Universidad Pontificia Comillas, Instituto de Investigación Tecnológica (IIT), ICAI School of Engineering, and Universidad de Jaen. Additionally, it is important to thanks NIST for making FDS available.

REFERENCES

- [1] NFPA92B. Guide for smoke management systems in atria, covered malls, and large areas. Quincy MA USA 2005.
- [2] Floyd, J., Forney, G., Hostikka, S., Korhonen, T., McDermott, R., McGrattan, K. Fire Dynamics Simulator (Version 6) User's Guide. Vol. 1. 1st ed. United States: National Institute of Standard and Technology; 2013.
- [3] Floyd, J., Forney, G., Hostikka, S., Korhonen, T., McDermott, R., McGrattan, K. Fire Dynamics Simulator (Version 6) Technical Reference Guide. vol. 1. 1st ed. United States: National Institute of Standard and Technology; 2013.
- [4] Engineers S of FP. SFPE. 3rd ed. Quincy, MA USA: National Fire Protection Association; 2002.
- [5] McGrattan KB, Baum HR, Rehm RG. Large eddy simulations of smoke movement. *Fire Saf J* 1998;30:161–78.
- [6] Siegel R, Howell JR. Thermal Radiation Heat Transfer. 4th ed. Taylor & Francis Inc; 2001.
- [7] Gutiérrez-Montes C, Sanmiguel-Rojas E, Viedma A, Rein G. Experimental data and numerical modelling of 1.3 and 2.3 MW fires in a 20 m cubic atrium. *Build Environ* 2009;44:1827–39.
- [8] Jarrin, N. Synthetic Inflow Boundary Conditions for the Numerical Simulation of Turbulence. PhD Thesis. The University of Manchester, 2008.
- [9] Cooper LY, Harkleroad M, Quintiere J, Rinkinen W. An Experimental Study of Upper Hot Layer Stratification in Full-Scale Multiroom Fire Scenarios. *J Heat Transf* 1982;104:741–9.
- [10] Quintiere JG, Steckler, K., Corley, D. An assessment of fire induced flows in compartments. *Fire Sci Technol* 1984;4:1–14.
- [11] Janssens M, Tran HC. Data Reduction of Room Tests for Zone Model Validation. *J Fire Sci* 1992;10:528–55.
- [12] He Y, Fernando A, Luo M. Determination of interface height from measured parameter profile in enclosure fire experiment. *Fire Saf J* 1998;31:19–38.